Experimental and Computational Multiphase Flow
Vol. 1, No. 2, 2019, 85–100
https://doi.org/10.1007/s42757-019-0009-y

One-dimensional drift-flux correlations for two-phase flow in medium-size channels

Takashi Hibiki (✉)

School of Nuclear Engineering, Purdue University, 400 Central Drive, West Lafayette, IN 47907-2017, USA

Abstract

The drift-flux parameters such as distribution parameter and drift velocity are critical parameters in the one-dimensional two-fluid model used in nuclear thermal-hydraulic system analysis codes. These parameters affect the drag force acting on the gas phase. The accurate prediction of the drift-flux parameters is indispensable to the accurate prediction of the void fraction. Because of this, the current paper conducted a state-of-the-art review on one-dimensional drift-flux correlations for various flow channel geometries and flow orientations. The essential conclusions were: (1) a channel geometry affected the distribution parameter, (2) a boundary condition (adiabatic or diabatic) affected the distribution parameter in a bubbly flow, (3) the drift velocity for a horizontal channel could be approximated to be zero, and (4) the distribution parameter developed for a circular channel was not a good approximation to calculate the distribution parameter for a sub-channel of the rod bundle. In addition to the above, the review covered a newly proposed concept of the two-group drift-flux model to provide the constitutive equation to close the modified gas mixture momentum equation of the two-fluid model mathematically. The review was also extended to the existing drift-flux correlations applicable to a full range of void fraction (Chexel–Lellouche correlation and Bhagwat–Ghajar correlation).

Keywords

drift-flux model
interfacial drag force
distribution parameter
nuclear thermal-hydraulic analysis
interfacial transport equation

Article History

Received: 7 January 2019
Revised: 6 February 2019
Accepted: 6 February 2019

Review Article

1 Introduction

Nuclear thermal-hydraulic safety analysis codes are used for safety analyses of nuclear power plants. Since the nuclear power plant is a large complex system, full three-dimensional computational fluid dynamic simulation is currently unrealistic due to an immense amount of computational time and unavailability of reliable local constitutive equations (Chuang and Hibiki, 2015, 2017; Vaidheeswaran and Hibiki, 2017). The current practice for simulating thermal-hydraulic behavior in the nuclear power plant system heavily depends on one-dimensional system analysis codes such as TRACE (Bajorek, 2008), RELAP5 (ISL, 2001), and TRAC (Borkowski et al., 1992) codes. These one-dimensional system analysis codes are architected through rigorous one-dimensional two-phase flow formulation such as the two-fluid model (Ishii and Hibiki, 2010). The two-fluid model is composed of mass, momentum, and energy balance equations for each phase. Kinematic and thermal non-equilibrium two-phase flow dynamics can be simulated through interfacial transfer terms in the two-fluid model. The kinematic non-equilibrium between two phases appears as a relative velocity between two phases, whereas the thermal non-equilibrium between two phases causes heat transfer through the interface between two phases. The interfacial drag force and heat transfer coefficient are two of the most critical terms which govern the kinematic and thermal non-equilibrium, respectively.

The interfacial drag force includes various terms such as Basset force, virtual mass force, drag force, lift force, wall lubrication force, turbulence dispersion force, bubble–bubble collision force, and wall-collision force (Chuang and Hibiki, 2017). In a one-dimensional simulation, the virtual mass force is vital for stabilizing the numerical simulation, whereas robust formulation of the drag force is a key to predict void fraction accurately. In the one-dimensional simulation, it is common to neglect the terms other than virtual mass force and drag force terms. The rigorous formulation of the drag force based on a drag coefficient includes an interfacial area concentration, which is one of the weakest links in constitutive equations to close the

The original version of this article was revised due to a retrospective Open Access order.

✉ hibiki@purdue.edu

two-fluid model mathematically. Unavailability of reliable constitutive equations for the prediction of the interfacial area concentration (Chuang and Hibiki, 2015) motivated developing an alternative method to formulate the one-dimensional drag force without the interfacial area concentration (Andersen and Chu, 1982). Andersen and Chu (1982) expressed the one-dimensional drag force through a drift velocity. This simplified approach has been extended for three-dimensional drag force formulation (Hibiki et al., 2018).

The one-dimensional drift-flux model plays a crucial role in the drag force formulation regardless of the formulation methodology (drag-coefficient-based formulation or drift-velocity-based formulation). The one-dimensional or area-averaged relative velocity appearing in the drag force is represented by void-fraction-weighted mean gas and liquid velocities, area-averaged void fraction, and distribution parameter (Ishii and Mishima, 1984). It has been pointed out that the area-averaged relative velocity formulation derived by Ishii and Mishima (1984) misses a void fraction or relative velocity covariance term (Brooks et al., 2012a). The constitutive equations of void fraction and relative velocity covariance terms have been developed for circular and sub-channel geometries (Hibiki and Ozaki, 2017; Ozaki and Hibiki, 2018). In the drift-velocity-based formulation, the overall drag coefficient is formulated through the drift velocity. The above brief discussion suggests the importance of constitutive equations for two drift-flux parameters such as distribution parameter and drift velocity.

The significance of the distribution parameter is the covariance of void fraction and mixture volumetric flux. The distribution parameter depending on flow channel geometry has been formulated empirically. The significance of the drift velocity is the difference between gas velocity and mixture volumetric flux. The drift velocity depending on the drag coefficient or bubble shape regime has been formulated with the aid of the drag law. Because of the importance of the constitutive equations for the drift-flux parameters in one-dimensional drag force formulation, a state-of-the-art review on one-dimensional drift-flux correlations for various flow channel geometries and flow orientations is conducted in this paper. Section 2 briefly describes the formulation of the one-dimensional drift-flux model and interfacial drag force using two drift-flux parameters such as distribution parameter and drift velocity. Section 3 reviews the state-of-the-art constitutive equations of the one-dimensional drift-flux model for two-phase flow in various medium-size channels. Section 4 covers a newly proposed concept of the two-group drift-flux model to provide the constitutive equation to close the modified gas mixture momentum equation mathematically. Section 5 describes existing drift-flux correlations applicable to a full range of void fraction.

2 Formulations of the drift-flux model and interfacial drag force

Zuber and Findlay (1965) proposed the drift velocity, v_{gj}, to consider the effect of the relative velocity between two phases, v_r, on the void fraction, α, as

$$v_{gj} \equiv v_g - j \tag{1}$$

where v_g and j are the gas velocity and mixture volumetric flux, respectively. Multiplying Eq. (1) by the void fraction and area-averaging the equation yields the one-dimensional drift-flux model as

$$\langle\langle v_g \rangle\rangle = C_0 \langle j \rangle + \langle\langle v_{gj} \rangle\rangle \tag{2}$$

where $\langle\ \rangle$ and $\langle\langle\ \rangle\rangle$ are the area-averaged and void-fraction-weighted mean quantities, respectively. The distribution parameter, C_0, and void-fraction-weighted mean drift velocity, $\langle\langle v_{gj} \rangle\rangle$, are defined as given by Eqs. (3) and (4), respectively.

$$C_0 \equiv \frac{\langle \alpha j \rangle}{\langle \alpha \rangle \langle j \rangle} \tag{3}$$

$$\langle\langle v_{gj} \rangle\rangle \equiv \frac{\langle \alpha v_{gj} \rangle}{\langle \alpha \rangle} \tag{4}$$

The one-dimensional form of the interfacial drag force, $\langle M_{ig}^{D} \rangle$, used in nuclear thermal-hydraulic safety analysis codes is expressed as

$$\langle M_{ig}^{D} \rangle = -\langle C_i \rangle |\langle v_r \rangle| \langle v_r \rangle \tag{5}$$

When the interfacial drag force is given by Andersen approach (Andersen and Chu, 1982) or drift-velocity-based formulation, the area-averaged drag coefficient, $\langle C_i \rangle$, is represented by

$$\langle C_i \rangle = \frac{\langle \alpha \rangle (1 - \langle \alpha \rangle)^3 \Delta\rho g}{\langle\langle v_{gj} \rangle\rangle^2} \tag{6}$$

where $\Delta\rho$ and g are the density difference between the two phases and gravitational acceleration, respectively.

The area-averaged relative velocity, $\langle v_r \rangle$, is formulated as

$$\langle v_r \rangle = C_\alpha' \left(\frac{1 - C_0 \langle \alpha \rangle}{1 - \langle \alpha \rangle} \langle\langle v_g \rangle\rangle - C_0 \langle\langle v_f \rangle\rangle \right) \tag{7}$$

where v_f is the liquid velocity. The relative velocity covariance, C_α', is defined by

$$C_\alpha' \equiv \frac{1 - \langle \alpha \rangle}{1 - C_\alpha \langle \alpha \rangle} \tag{8}$$

where the void fraction covariance, C_α, is defined by

$$C_\alpha \equiv \frac{\langle \alpha^2 \rangle}{\langle \alpha \rangle^2} \tag{9}$$

It should be noted here that current nuclear thermal-hydraulic safety analysis codes based on Ishii–Mishima formulation (1984) ignore the relative velocity covariance in Eq. (7).

When the interfacial drag force is formulated through the drag coefficient, C_D (drag-coefficient-based formulation), the area-averaged drag coefficient, $\langle C_i \rangle$, is represented by

$$\langle C_i \rangle = \frac{1}{8} C_D \langle a_i \rangle \rho_f \tag{10}$$

where a_i and ρ_f are the interfacial area concentration and liquid density, respectively.

As briefly described above, two drift-flux parameters such as the distribution parameter and void-fraction-weighted mean drift velocity (hereafter drift velocity for simplicity) are required for formulating the one-dimensional drag force. In what follows, the state-of-the-art review on constitutive equations of the drift-flux model for medium-size channels is presented.

3 Constitutive equations of the drift-flux model for medium-size channels

3.1 Upward two-phase flow in a vertical circular channel

The distribution parameter and drift velocity are in general dependent on flow regime. Before a drift-flux correlation is applied to upward two-phase flow in a vertical circular channel, the flow regime should be identified. There are several reliable flow regime transition criteria for upward two-phase flow in a vertical circular channel (Taitel et al., 1980; Mishima and Ishii, 1984).

The drift velocity of dispersed two-phase flow can be modeled by the drag law. Ishii (1977) summarized the drift velocity correlations for upward two-phase flow in a vertical circular channel as follows.

Bubbly flow:

$$\langle\langle v_{gj} \rangle\rangle = \sqrt{2}\left(\frac{\Delta\rho g \sigma}{\rho_f^2}\right)^{0.25} (1-\langle \alpha \rangle)^{1.75} \tag{11}$$

where σ is the surface tension.

Slug flow:

$$\langle\langle v_{gj} \rangle\rangle = 0.35\left(\frac{\Delta\rho g D}{\rho_f}\right)^{0.5} \tag{12}$$

where D is the channel diameter.

Churn flow:

$$\langle\langle v_{gj} \rangle\rangle = \sqrt{2}\left(\frac{\Delta\rho g \sigma}{\rho_f^2}\right)^{0.25} \tag{13}$$

The distribution parameter correlation for upward adiabatic two-phase flow in a vertical circular channel is given by

$$C_0 = 1.2 - 0.2\sqrt{\frac{\rho_g}{\rho_f}} \tag{14}$$

where ρ_g is the gas density. Although Eq. (14) is applicable to slug and churn flow regimes, it does not consider the complicated phase distribution mechanism observed in bubbly flow regime. The phase distribution is primarily governed by local non-drag forces such as lift, wall-lubrication, turbulence dispersion, bubble–bubble collision, and bubble–wall collision forces (Chuang and Hibiki, 2017). Hibiki and Ishii (2002a) calculated the distribution parameter from measured profiles of local void fraction and local gas and liquid velocities, and found the dependence of the distribution parameter on the bubble Sauter mean diameter. They developed the distribution parameter correlation for upward adiabatic bubbly flow in a vertical circular channel as

$$C_0 = \left(1.2 - 0.2\sqrt{\frac{\rho_g}{\rho_f}}\right)\left[1-\exp\left(-22\frac{\langle D_{Sm} \rangle}{D}\right)\right] \tag{15}$$

where D_{Sm} is the bubble Sauter mean diameter, which can be calculated by Hibiki–Ishii correaltion (2002b). Equation (15) has been validated by the atmospheric bubbly flow data taken in circular channels with the inner diameter ranging from 25.4 to 60.0 mm. The distribution parameter correlation for subcooled bubbly flow is given by

$$C_0 = \left(1.2 - 0.2\sqrt{\frac{\rho_g}{\rho_f}}\right)[1-\exp(-18\langle \alpha \rangle)] \tag{16}$$

The drift velocity of separated two-phase flow such as pure annular flow cannot be defined locally because the local flow is either gas single-phase or liquid single-phase. In this case, the drift-flux model is formulated through the force balance between liquid film and gas core. For annular flow, the drift-flux correlation is given in the form of mean drift velocity, $\overline{V_{gj}}$, as

$$\overline{V_{gj}} \approx \frac{1-\langle \alpha \rangle}{\langle \alpha \rangle + \left[\frac{1+75(1-\langle \alpha \rangle)}{\sqrt{\langle \alpha \rangle}}\frac{\rho_g}{\rho_f}\right]^{1/2}}\left[\langle j \rangle + \sqrt{\frac{\Delta\rho g D(1-\langle \alpha \rangle)}{0.015\rho_f}}\right] \tag{17}$$

which is further simplified for $\rho_g/\rho_f \ll 1$ as

$$\overline{V_{gj}} \approx \frac{1-\langle \alpha \rangle}{\langle \alpha \rangle + 4\sqrt{\rho_g/\rho_f}}\left[\langle j \rangle + \sqrt{\frac{\Delta\rho g D(1-\langle \alpha \rangle)}{0.015\rho_f}}\right] \tag{18}$$

In a strict sense, the distribution parameter and drift velocity should be experimentally obtained from Eqs. (3) and (4) with measured profiles of local void fraction and gas and liquid velocities to validate the above correlations. Limited availability of the measured profiles only allows for the rigorous validation of Eqs. (11) and (15) as shown in Fig. 1 (Hibiki and Ishii, 2002a). The validation for other cases relies on a drift-flux plot ($\langle j \rangle$ vs. $\langle\langle v_g \rangle\rangle$ plot). The prediction error is estimated for a set of distribution parameter and drift velocity correlations. Ishii (1977) showed the validity of the drift-flux correlation for air–water, boiling Freon-22, boiling water, and boiling heavy water systems under the conditions of $\rho_g/\rho_f \le 0.16$ and the pipe diameter up to 168 mm. The constitutive equations described in Section 3.1 have been widely accepted and implemented into nuclear thermal-hydraulic safety analysis codes.

3.2 Upward two-phase flow in a vertical rectangular channel

The distribution parameter and drift velocity are in general dependent on flow regime. Before a drift-flux correlation is applied to upward two-phase flow in a vertical rectangular channel, the flow regime should be identified. A reliable model of flow regime transition criteria for upward two-phase flow in a vertical rectangular channel is available (Hibiki and Mishima, 2001).

The distribution parameter correlations for adiabatic and subcooled boiling flows are expressed as given in Eqs. (19) and (20), respectively (Ishii, 1977).

$$C_0 = 1.35 - 0.35\sqrt{\frac{\rho_g}{\rho_f}} \tag{19}$$

$$C_0 = \left(1.35 - 0.35\sqrt{\frac{\rho_g}{\rho_f}}\right)\left[1 - \exp(-18\langle\alpha\rangle)\right] \tag{20}$$

The applicability of Eqs. (19) and (20) to a rectangular channel with the aspect ratio of the order of unity, namely nearly a square channel has not been confirmed. When the aspect ratio of a rectangular channel is unity, a round channel may be an assumption better than a rectangular channel with a certain aspect ratio. The distribution parameters for a circular channel, Eqs. (14) and (16), are lower than those for a rectangular channel, Eqs. (19) and (20). It is expected that the distribution parameter for a rectangular channel may decrease as the aspect ratio approaches unity. Due to the lack of detailed local flow parameters such as void fraction and gas and liquid velocities in a rectangular channel, the distribution parameter determined through Eq. (3) does not exist. The distribution parameter correlation for an adiabatic bubbly flow in a rectangular channel is not available.

The drift velocity correlations for dispersed flow regimes, Eqs. (11), (12), and (13), were developed based on local drag law depending on a bubble shape regime, similarity hypothesis between a single-particle system and a multi-particle system, and simplification to replace local void fraction with an area-averaged void fraction (Ishii, 1977). These assumptions are not susceptible to a medium-size channel geometry. The drift velocity correlations recommended for a circular channel, Eqs. (11), (12), (13), and (17), are applied to a rectangular channel. Figure 2 compares the drift-flux correlation, Eqs. (13) and (19), with the data taken in a rectangular channel under the pressure ranging from 0.789 to 4.23 MPa (Abbs and Hibiki, 2019). Ishii (1977) showed the validity of the drift-flux correlation for boiling water, boiling R-11, and nitrogen–NaK systems under the conditions of $\rho_g/\rho_f \le 0.04$ and the aspect ratio ranging from 2.8 to 9.4.

3.3 Upward two-phase flow in vertical annulus channel

The distribution parameter and drift velocity are in general dependent on flow regime. Before a drift-flux correlation is applied to upward two-phase flow in a vertical annulus

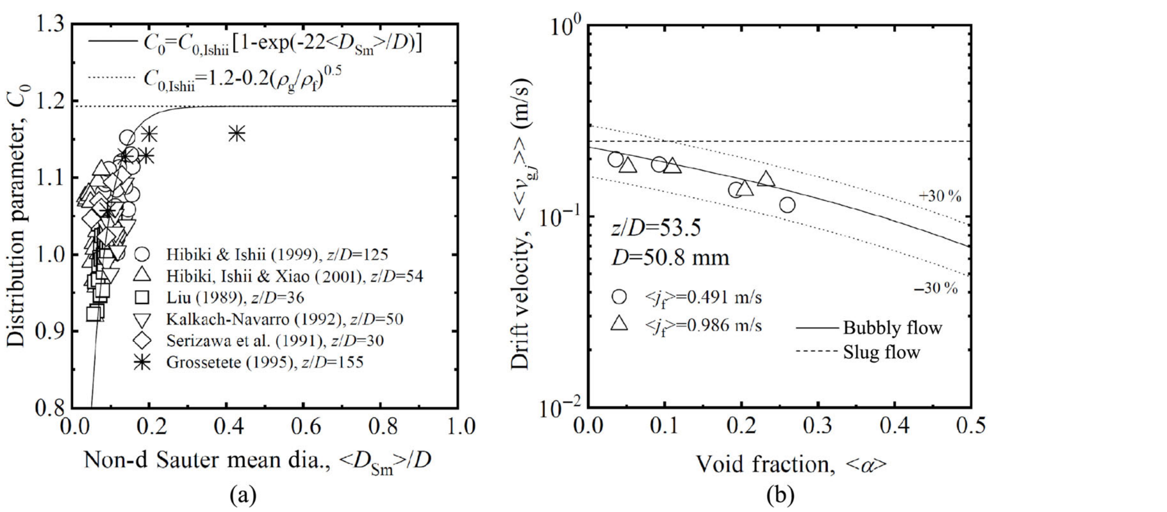

Fig. 1 Validation of distribution parameter and void fraction correlations for a circular channel (Hibiki and Ishii, 2002b; reproduced with permission © Elsevier Science Ltd. 2002).

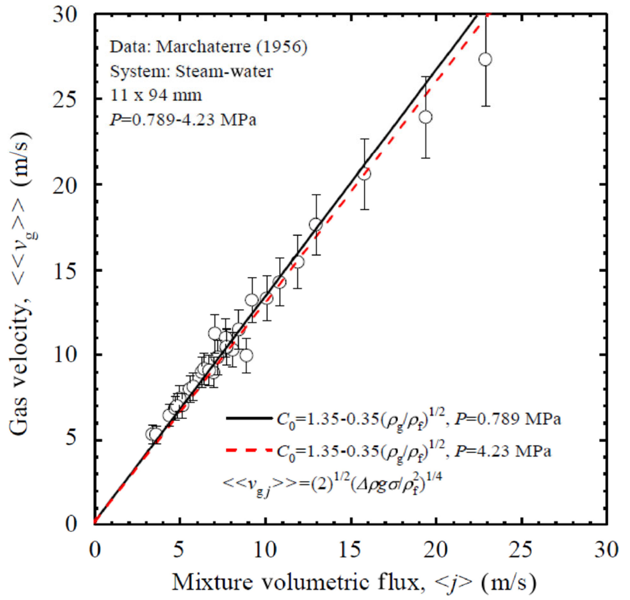

Fig. 2 Comparison of drift-flux correlation with the data taken in a rectangular channel under the pressure ranging from 0.789 to 4.23 MPa (Abbs and Hibiki, 2019; reproduced with permission © Elsevier Ltd. 2018).

channel, the flow regime should be identified. A reliable model of flow regime transition criteria for upward two-phase flow in a vertical annulus channel is available (Julia and Hibiki, 2011).

Equation (14) has been utilized for predicting the distribution parameter for upward adiabatic two-phase flow in a vertical annulus channel. Ozar et al. (2008) calculated the distribution parameter with the profiles of measured local void fraction, assumed local mixture volumetric flux, and proposed the following distribution parameter correlation for upward adiabatic bubbly flow in a vertical annulus channel.

$$C_0 = \left(1.1 - 0.1\sqrt{\frac{\rho_g}{\rho_f}}\right)\left[1 - \exp\left(-22\frac{\langle D_{Sm}\rangle}{D_H}\right)\right] \tag{21}$$

where D_H is the hydraulic equivalent diameter.

For a higher void fraction, the distribution parameter is given by

$$C_0 = 1.1 - 0.1\sqrt{\frac{\rho_g}{\rho_f}} \tag{22}$$

Equation (21) indicates that the distribution parameters for an annulus channel, Eqs. (21) and (22), are smaller than those for a circular channel, Eqs. (14) and (15). This has been explained through Eq. (3) with assumed power-law profiles of local void fraction and mixture volumetric flux (Ozar et al., 2008).

Hibiki et al. (2003) developed the bubble-layer thickness model to predict the distribution parameter for subcooled boiling flow in a vertical annulus channel. The distribution parameter correlation is analytically derived with the assumed distribution parameter for saturated boiling flow, Eq. (14), as

$$C_0 = \left(1.2 - 0.2\sqrt{\frac{\rho_g}{\rho_f}}\right)\left[1 - \exp(-3.12\langle\alpha\rangle^{0.212})\right] \tag{23}$$

Brooks et al. (2012b) modified Eq. (23) with the assumed distribution parameter for saturated boiling flow, Eq. (22), as

$$C_0 = \left(1.1 - 0.1\sqrt{\frac{\rho_g}{\rho_f}}\right)\left[1 - \exp(-5.76\langle\alpha\rangle^{0.248})\right] \tag{24}$$

Figures 3(a) and 3(b) compare Eqs. (21) and (24) with the

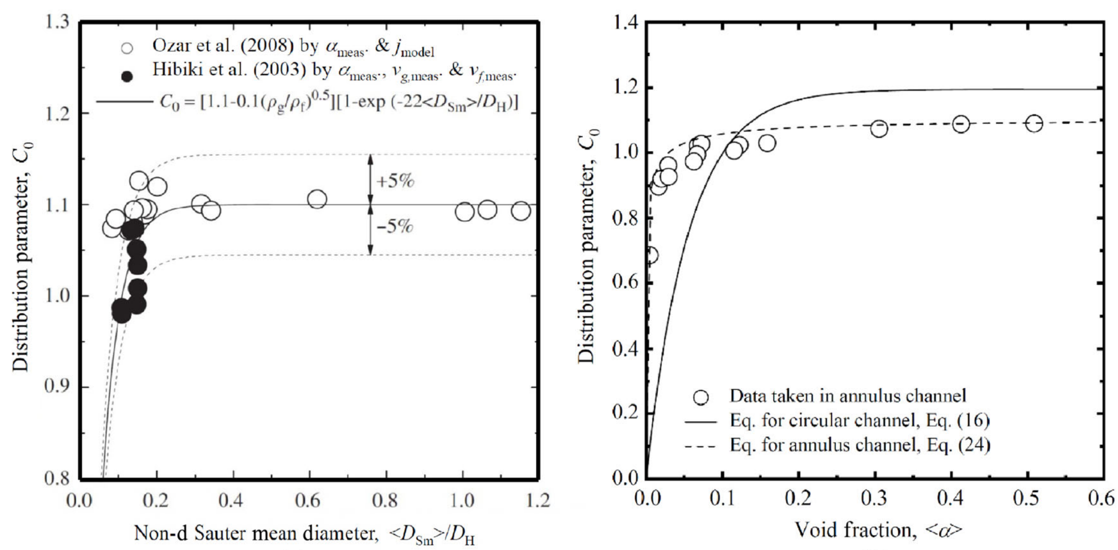

(a) (b)

Fig. 3 Validation of distribution parameter correlations for (a) adiabatic and (b) boiling flows in annulus channels (Ozar et al., 2008; reproduced with permission © Elsevier Ltd. 2008).

data taken for upward adiabatic and boiling flows in vertical annuli, respectively. Equations (21) and (24) have been respectively validated by the atmospheric and boiling bubbly flow data taken in annulus channels with the rod diameter of 19.1 mm and the inner diameter of the outer pipe being 38.1 mm.

As discussed in Section 3.2, the drift velocity correlations recommended for a circular channel, Eqs. (11), (12), (13), and (17), are applied to an annulus channel.

3.4 Upward two-phase flow in a vertical sub-channel of rod bundle geometry

The distribution parameter and drift velocity are in general dependent on flow regime. Before a drift-flux correlation is applied to upward two-phase flow in a vertical sub-channel of the rod bundle geometry, the flow regime should be identified. A reliable model of flow regime transition criteria for upward two-phase flow in a vertical sub-channel of the rod bundle geometry is available (Liu and Hibiki, 2017).

Julia et al. (2009) analytically derived the distribution parameter for upward subcooled boiling flow in a vertical sub-channel of the rod bundle geometry using the bubble layer thickness model (Hibiki et al., 2003) as

$$C_0=\begin{cases}\left(1.03-0.03\sqrt{\dfrac{\rho_g}{\rho_f}}\right)\left[1-\exp\left(-26.3\langle\alpha\rangle^{0.780}\right)\right], & D_0/P_0=0.3\\ \left(1.04-0.04\sqrt{\dfrac{\rho_g}{\rho_f}}\right)\left[1-\exp\left(-21.1\langle\alpha\rangle^{0.762}\right)\right], & D_0/P_0=0.5\\ \left(1.05-0.05\sqrt{\dfrac{\rho_g}{\rho_f}}\right)\left[1-\exp\left(-34.1\langle\alpha\rangle^{0.925}\right)\right], & D_0/P_0=0.7\end{cases} \tag{25}$$

where D_0 and P_0 are the rod diameter and rod pitch, respectively. Julia et al. (2009) recommended the following drift velocity correlation modified for a confined channel to be used together with Eq. (25) in bubbly flow regime.

$$\langle\langle v_{gj}\rangle\rangle=\sqrt{2}\left(\frac{\Delta\rho g\sigma}{\rho_f^2}\right)^{0.25}(1-\langle\alpha\rangle)^{1.75}B_{sf} \tag{26}$$

where B_{sf} is the bubble size factor to consider the rod wall effect on the bubble rising velocity.

$$B_{sf}=\begin{cases}1-\dfrac{D_b}{0.9\left(\sqrt{2}P_0-2R_0\right)}, & \text{for } \dfrac{D_b}{\sqrt{2}P_0-2R_0}<0.6\\ 0.12\left(\dfrac{D_b}{\sqrt{2}P_0-2R_0}\right)^{-2}, & \text{for } \dfrac{D_b}{\sqrt{2}P_0-2R_0}\geq 0.6\end{cases} \tag{27}$$

Ozaki and Hibiki (2015) developed the distribution parameter correlation for upward boiling two-phase flow in a vertical 8×8 rod bundle under prototypic pressure and temperature conditions of a nuclear reactor as

$$C_0=1.1-0.1\sqrt{\frac{\rho_g}{\rho_f}} \tag{28}$$

Equation (28) is applicable to the void fraction of 0.87. Equation (28) is optimized with the use of Hibiki–Ishii's drift velocity correlation (Hibiki and Ishii, 2003) given by

$$V_{gj}^{+}=V_{gj,B}^{+}\exp\left(-1.39\langle j_g^{+}\rangle\right)+V_{gj,P}^{+}\left[1-\exp\left(-1.39\langle j_g^{+}\rangle\right)\right] \tag{29}$$

where V_{gj}^{+} and $\langle j_g^{+}\rangle$ are, respectively, the non-dimensional drift velocity and superficial gas velocity defined by

$$V_{gj}^{+}\equiv\frac{\langle\langle v_{gj}\rangle\rangle}{\left(\dfrac{\Delta\rho g\sigma}{\rho_f^2}\right)^{0.25}},\quad \langle j_g^{+}\rangle\equiv\frac{\langle j_g\rangle}{\left(\dfrac{\Delta\rho g\sigma}{\rho_f^2}\right)^{0.25}} \tag{30}$$

The subscripts of B and P are the drift velocity for bubbly flow calculated by Eq. (11) and pool condition calculated by Kataoka–Ishii correlation (1987), respectively. Figure 4 compares the drift-flux correlation, Eqs. (28) and (29), with the data taken in a vertical 8×8 rod bundle under the pressure of 7.2 MPa (Ozaki and Hibiki, 2015). Equations (28) and (29) have been validated by NUPEC BTBF data (Morooka et al., 1991), JAERI TPTF data (Kondo et al., 1993), and Purdue adiabatic data (Yang et al., 2012). The applicable range covers the pressure from 0.1 to 11.8 MPa, mass velocity from 5 to 2000 kg/(m²·s), hydraulic equivalent diameter from 9.8 to 21.7 mm, and casing size from 79 to 140 mm (Ozaki et al., 2013).

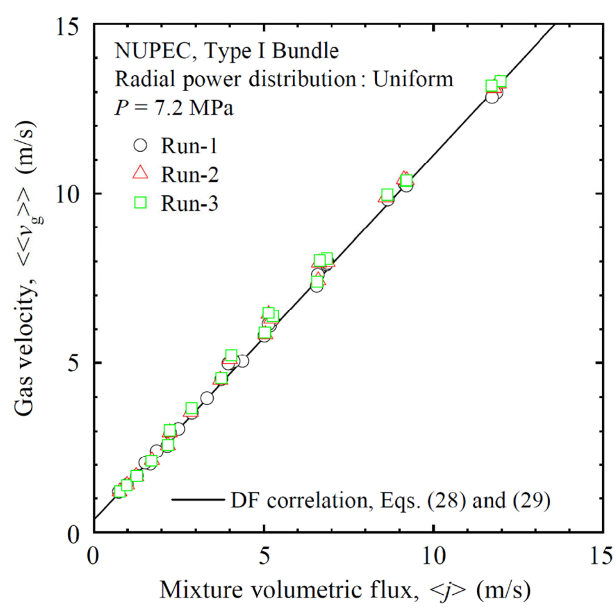

Fig. 4 Comparison of drift-flux correlation with the data taken in a 8×8 rod bundle under the pressure of 7.2 MPa (Ozaki and Hibiki, 2015; reproduced with permission © Elsevier Ltd. 2015).

Ozaki and Hibiki (2018) modified Eq. (25) to match with Eq. (28) for a high void fraction and analytically derived the distribution parameter for upward subcooled boiling flow in a vertical sub-channel of the rod bundle geometry as

$$C_0 = \left(1.1 - 0.1\sqrt{\frac{\rho_g}{\rho_f}}\right)[1 - \exp(-12.1\langle\alpha\rangle^{0.701})], \quad D_0/P_0 = 0.7 - 0.9 \tag{31}$$

Liu et al. (2018) empirically developed the distribution parameter correlation for upward adiabatic bubbly flow in a vertical 5×5 rod bundle as

$$C_0 = \left(1.1 - 0.1\sqrt{\frac{\rho_g}{\rho_f}}\right)\left[1 - \exp\left(-17\frac{\langle D_{Sm}\rangle}{D_H}\right)\right] \tag{32}$$

Equation (32) has been validated by the data taken for upward adiabatic bubbly flow in a vertical 5×5 rod bundle under the atmospheric condition.

3.5 Horizontal two-phase flow in a circular channel

The distribution parameter and drift velocity are in general dependent on flow regime. Before a drift-flux correlation is applied to horizontal two-phase flow, the flow regime should be identified. The flow regime transition criteria for horizontal two-phase flow are rather complicated because the flow regime for horizontal gas–liquid two-phase flow is susceptible to inlet conditions and developing length. Because the flow regime transition criteria for horizontal two-phase flow have not been well-developed (Barnea et al., 1980), a general drift-flux correlation applicable to the full-range of the void fraction has been developed by Rassame and Hibiki (2018).

The buoyancy force acting on the gas phase is perpendicular to the flow direction resulting in no relative velocity or drift velocity along the flow direction.

$$\langle\langle v_{gj}\rangle\rangle = 0 \text{ m/s} \tag{33}$$

The distribution parameter correlation for horizontal two-phase flow is given by

$$\begin{aligned} C_0 &= 0.800\left[0.815\left(\frac{\langle j_g^+\rangle/\langle j^+\rangle}{0.900}\right)^{1.50}\right] \\ &\quad - \left\{0.800\left[0.815\left(\frac{\langle j_g^+\rangle/\langle j^+\rangle}{0.900}\right)^{1.50}\right] - 1\right\}\sqrt{\frac{\rho_g}{\rho_f}}, \\ &\quad \text{for } 0 \le \langle j_g^+\rangle/\langle j^+\rangle < 0.9; \\ C_0 &= \left(-8.08\langle j_g^+\rangle/\langle j^+\rangle + 9.08\right) \\ &\quad - 8.08\left(\langle j_g^+\rangle/\langle j^+\rangle + 1\right)\sqrt{\frac{\rho_g}{\rho_f}}, \\ &\quad \text{for } 0.9 \le \langle j_g^+\rangle/\langle j^+\rangle \le 1 \end{aligned} \tag{34}$$

where

$$\langle j^+\rangle \equiv \frac{\langle j\rangle}{\left(\frac{\Delta\rho g\sigma}{\rho_f^2}\right)^{0.25}} \tag{35}$$

Figure 5 compares the drift-flux correlation, Eqs. (33) and (34), with the data taken in horizontal channels (Rassame and Hibiki, 2018). Equations (33) and (34) have been validated by the data taken for adiabatic air–water and air–kerosene flows in horizontal channels. The applicable range covers the superficial gas velocity from 0.0253 to 47.5 m/s, superficial liquid velocity from 5.7×10^{-5} to 5.97 m/s, and the channel diameter from 19 to 77.9 mm.

Baotong et al. (2019) developed an empirical drift-flux correlation for oil–water two-phase flow in horizontal channels as

$$\langle\langle v_o\rangle\rangle = 1.05\langle j\rangle \tag{36}$$

where $\langle\langle v_o\rangle\rangle$ is the oil-fraction-weighted mean oil velocity. Equation (36) has been validated by the data taken for adiabatic oil–water flows in horizontal channels. The applicable range covers the superficial oil velocity from 0.01 to 2.69 m/s, superficial water velocity from 0.01 to 2.7 m/s, and the channel diameter from 20 to 106 mm. The physical properties of the fluids in the database are the oil density from 787 to 998 kg/m^3, water density from 980 to 1000 kg/m^3, oil viscosity from 1.2 to 280 mPa·s, water viscosity from 0.84 to 1 mPa·s, and surface tension from 28 to 45 mN/m.

3.6 Downward two-phase flow in a vertical circular channel

The distribution parameter and drift velocity are in general dependent on flow regime. Before a drift-flux correlation is applied to downward two-phase flow in a vertical circular channel, the flow regime should be identified. The flow regime transition criteria for downward two-phase flow are rather complicated because the flow regime for downward two-phase flow is susceptible to buoyancy force acting in the opposite direction of the liquid flow. Because the flow regime transition criteria for downward two-phase flow in a vertical circular channel have not been well-developed (Lokanathan and Hibiki, 2018), a general drift-flux correlation applicable to the full-range of the void fraction has been developed by Goda et al. (2003).

To develop a general drift-flux correlation independent on the flow regime, the drift velocity is approximated by

$$\langle\langle v_{gj}\rangle\rangle = \sqrt{2}\left(\frac{\Delta\rho g\sigma}{\rho_f^2}\right)^{0.25} \tag{37}$$

The distribution parameter correlation for downward

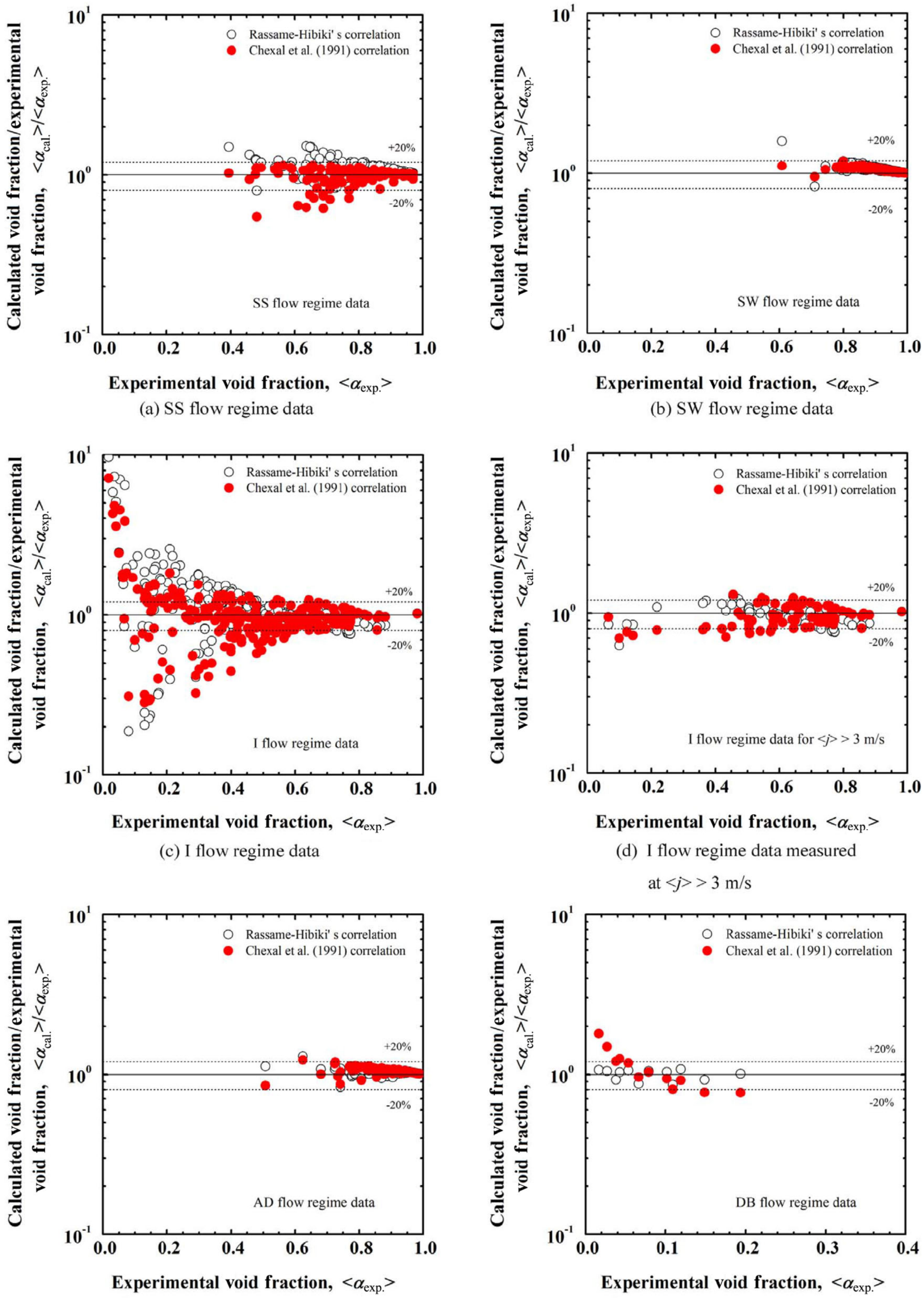

(a) SS flow regime data
(b) SW flow regime data
(c) I flow regime data
(d) I flow regime data measured at $<j> > 3$ m/s
(e) AD flow regime data
(f) DB flow regime data

Fig. 5 Comparison of drift-flux correlation, Eqs. (33) and (34), with the data taken in horizontal channels (SS: stratified smooth, SW: stratified wavy, I: intermittent, AD: annular flow with dispersed liquid droplets, DB: dispersed bubble) (Rassame and Hibiki, 2018; reproduced with permission © Elsevier Inc. 2017).

two-phase flow in a vertical circular channel is expressed by

$$\begin{aligned} C_0 &= (-0.0214\langle j^*\rangle + 0.772) \\ &\quad + (0.0214\langle j^*\rangle + 0.228)\sqrt{\frac{\rho_g}{\rho_f}}, \\ &\quad \text{for } -20 \le \langle j^*\rangle < 0; \\ C_0 &= \{0.2\exp[0.00848(\langle j^*\rangle + 20)] + 1.0\} \\ &\quad - 0.2\exp[0.00848(\langle j^*\rangle + 20)]\sqrt{\frac{\rho_g}{\rho_f}}, \\ &\quad \text{for } \langle j^*\rangle \le -20 \end{aligned} \tag{38}$$

where

$$\langle j^*\rangle \equiv \frac{\langle j\rangle}{\sqrt{2}\left(\dfrac{\Delta\rho g\sigma}{\rho_f^2}\right)^{0.25}} \tag{39}$$

Figure 6 compares the drift-flux correlation, Eqs. (37) and (38), with the data taken for downward two-phase flow in vertical circular channels (Goda et al., 2003). Equations (37) and (38) have been validated by the data taken for downward air–water and steam–water flows in vertical circular channels. The applicable range covers the mixture volumetric flux from –0.45 to –24.6 m/s, pressure from 0.1 to 1.5 MPa, and the channel diameter from 16 to 102.3 mm.

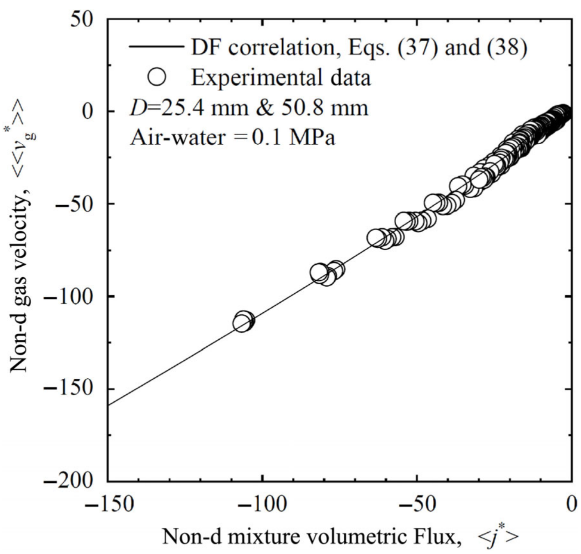

Fig. 6 Comparison of drift-flux correlation with the data taken for downward two-phase flow in vertical circular channels (Goda et al., 2003; reproduced with permission © Elsevier Ltd. 2003).

4 Constitutive equations of the two-group drift-flux model for medium-size channels

4.1 Basic concept of two-group drift-flux model

The concept of the two-group drift-flux model has been proposed to close the one-dimensional modified two-fluid model (Ishii and Hibiki, 2010). The two-group approach treats a bubble in two groups, namely, group-1 bubbles (spherical or distorted bubbles) and group-2 bubbles (cap or slug bubbles). The drag coefficient and interfacial area concentration available to mass, momentum, and heat transfers are dependent on the bubble shape regime. Two-group interfacial area transport equation has been proposed to enhance the prediction accuracy of the interfacial area concentration which affects the prediction accuracy of the interfacial drag force (Hibiki and Ishii, 2009). The introduction of the two-group interfacial area transport equation into the two-fluid model requires two gas continuity equation and two gas momentum equations resulting in 8 equation-based two-fluid model. To avoid the additional computational burden and numerical instability in the computation, the modified two-fluid model has been proposed to simplify the two gas momentum equations into a gas mixture momentum equation while still preserving the ability to treat the two bubble groups separately. The one-dimensional form of the mixture gas momentum equation in the modified two-fluid model is expressed as

$$\begin{aligned} &\frac{\partial}{\partial t}(\langle\alpha\rangle\rho_g\langle\langle v_g\rangle\rangle) + \frac{\partial}{\partial z}(\langle\alpha\rangle\rho_g\langle\langle v_g\rangle\rangle^2) \\ &= \langle\alpha\rangle\frac{\partial}{\partial z}\langle\langle P_g\rangle\rangle + \frac{\partial}{\partial z}(\langle\alpha\rangle\langle\langle\tau_{gzz} + \tau_{gzz}^T\rangle\rangle) - \langle\alpha\rangle\rho_g g - \frac{4\alpha_w\tau_{gw}}{D} \\ &\quad + \left\langle(P_{gi} - P_g)\frac{\partial\alpha}{\partial z}\right\rangle + \langle\Gamma_{g1}\rangle\langle\langle v_{g1}\rangle\rangle_1 + \langle\Gamma_{g2}\rangle\langle\langle v_{g2}\rangle\rangle_2 \\ &\quad + \langle M_{ig1}^D\rangle + \langle M_{ig2}^D\rangle - \frac{\partial}{\partial z}\left(\rho_g\frac{\langle\alpha_1\rangle\langle\alpha_2\rangle}{\langle\alpha\rangle}\overline{V_{g21}}^2\right) \\ &\quad + \langle\Delta\dot{m}_{12}\rangle\overline{V_{g21}} - \frac{\partial}{\partial z}\sum_{k=1}^{2}COV(\alpha_k\rho_g v_{gk}v_{gk}) \end{aligned} \tag{40}$$

where P, τ, τ^T, Γ, and $\Delta\dot{m}_{12}$ are the pressure, viscous shear stress, turbulent shear stress, mass generation rate per unit mass, and intergroup mass transfer rate per unit mass, respectively. The subscripts of w, i, 1, 2, and k are the wall, interface between two phases, group-1 bubble, group-2 bubble, and group-k bubble, respectively. The difference between the phase-fraction-weighted mean velocities, $\overline{V_{g21}}$, is defined by

$$\overline{V_{g21}} = \langle\langle v_{g2}\rangle\rangle_2 - \langle\langle v_{g1}\rangle\rangle_1 \tag{41}$$

where

$$\langle\langle v_{gk}\rangle\rangle_k \equiv \frac{\langle\alpha_k v_{gk}\rangle}{\langle\alpha_k\rangle} \tag{42}$$

To close the one-dimensional modified two-fluid model, the closure relationships for $\langle\langle v_{g1}\rangle\rangle$ and $\langle\langle v_{g2}\rangle\rangle$ should be given though the two-group drift-flux model expressed by

$$\langle\langle v_{gk}\rangle\rangle_k = C_{0k}\langle j\rangle + \langle\langle v_{gjk}\rangle\rangle_k \tag{43}$$

where

$$C_{0k} = \frac{\langle \alpha_k j\rangle}{\langle \alpha_k\rangle\langle j\rangle} \tag{44}$$

and

$$\langle\langle v_{gjk}\rangle\rangle_k \equiv \frac{\langle (v_{gk} - j)\alpha_k\rangle}{\langle \alpha_k\rangle} \tag{45}$$

The distribution parameter and void-fraction-weighted mean drift velocity can be expressed by the distribution parameters and drift velocities for group-1 and group-2 as

$$C_0 = \frac{\sum_{k=1}^{2} C_{0k}\langle \alpha_k\rangle}{\sum_{k=1}^{2}\langle \alpha_k\rangle} \tag{46}$$

and

$$\langle\langle v_{gj}\rangle\rangle = \frac{\sum_{k=1}^{2}\langle\langle v_{gjk}\rangle\rangle_k\langle \alpha_k\rangle}{\sum_{k=1}^{2}\langle \alpha_k\rangle} \tag{47}$$

4.2 Upward adiabatic two-phase flow in a vertical annulus channel

Brooks et al. (2012c) recommended Eqs. (48) and (49) for the distribution parameters of group-1 and group-2 bubbles of upward adiabatic two-phase flow in a vertical annulus channel.

$$C_{01} = \left(1.1 - 0.1\sqrt{\frac{\rho_g}{\rho_f}}\right)\left[1 - \exp\left(-22\frac{\langle D_{Sm,1}\rangle}{D_H}\right)\right] \tag{48}$$

and

$$C_{02} = 1.1 - 0.1\sqrt{\frac{\rho_g}{\rho_f}} \tag{49}$$

Figures 7(a) and 7(b) compare Eqs. (48) and (49) with the group-1 and group-2 bubble data taken for upward adiabatic two-phase flows in vertical annulus channels, respectively. Equations (48) and (49) have been validated by the data taken in upward adiabatic air–water flow in a vertical annulus channel under the pressure from 0.12 to 0.6 MPa.

The drift velocity for a group-1 bubble is given by

$$\langle\langle v_{gj1}\rangle\rangle_1 = \sqrt{2}\left(\frac{\Delta\rho g\sigma}{\rho_f^2}\right)^{0.25}(1 - \langle \alpha_1\rangle)^{1.75} \tag{50}$$

The drift velocity for a group-2 bubble in a channel with a width, w, smaller than 52 times Laplace length is given as follows.

Cap bubbly flow ($w \ge (6t\langle D_{Sm,2}\rangle)/(2.7t - \langle D_{Sm,2}\rangle)$):

$$\langle\langle v_{gj2}\rangle\rangle_2 = 0.762\sqrt{\frac{\Delta\rho g}{\rho_f}\frac{t\langle D_{Sm,2}\rangle}{\langle t - 0.37\langle D_{Sm,2}\rangle\rangle}}(1 - \langle \alpha_2\rangle)^{1.5} \tag{51}$$

where t is the channel thickness.

Slug flow ($w < (6t\langle D_{Sm,2}\rangle)/(2.7t - \langle D_{Sm,2}\rangle)$):

$$\langle\langle v_{gj}\rangle\rangle = 0.35\left(\frac{\Delta\rho g D_H}{\rho_f}\right)^{0.5} \tag{52}$$

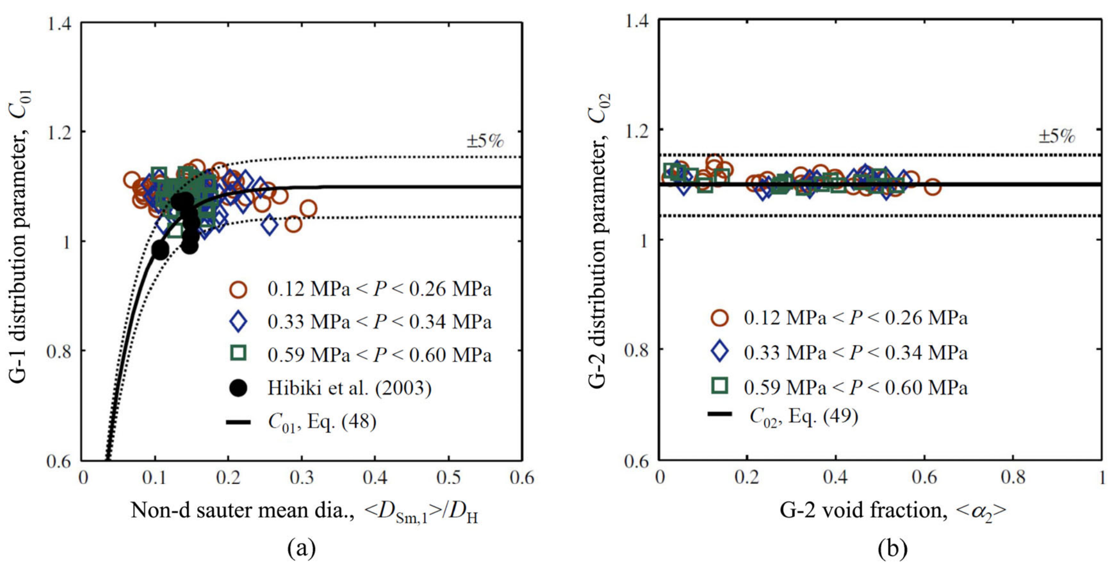

Fig. 7 Validation of adiabatic distribution parameter correlations for (a) group-1 bubbles and (b) group-2 bubbles in annulus channels (Brooks et al., 2012c; reproduced with permission © Elsevier Inc. 2012).

Churn flow:

$$\langle\langle v_{gj}\rangle\rangle=\sqrt{2}\left(\frac{\Delta\rho g\sigma}{\rho_f^2}\right)^{0.25}(1-\langle\alpha_2\rangle)^{0.25} \quad (53)$$

It should be noted here that the void fraction for group-1 bubble and Sauter mean diameter for group-2 bubble in a medium-size channel can be estimated by a constitutive correlation (Ozar et al., 2012).

4.3 Upward boiling two-phase flow in a vertical annulus channel

Brooks et al. (2012b) recommended Eqs. (54) and (55) for the distribution parameters of group-1 and group-2 bubbles of upward boiling two-phase flow in an annulus channel.

$$C_{01}=\left(1.1-0.1\sqrt{\frac{\rho_g}{\rho_f}}\right)\left[1-\exp\left(-5.76\langle\alpha_1\rangle^{0.248}\right)\right] \quad (54)$$

and

$$C_{02}=1.1-0.1\sqrt{\frac{\rho_g}{\rho_f}} \quad (55)$$

Figures 8(a) and 8(b) compare Eqs. (54) and (55) with the group-1 and group-2 bubble data taken for upward boiling two-phase flows in a vertical annulus, respectively. Equations (54) and (55) have been validated by the data taken in upward boiling steam–water flow in a vertical annulus channel under the pressure from 0.18 to 0.95 MPa.

The drift velocity correlations given in Section 4.2 can be used for upward boiling two-phase flow in a vertical annulus channel.

5 General drift-flux correlation applicable to full void fraction range

5.1 Chexel–Lellouche correlation

Chexel–Lellouche correlation also known as EPRI correlation has been implemented into RELAP5 code (ISL, 2001). The unique features of the Chexel–Lellouche correlation are (1) the independence on flow regime, (2) the applicability to the full range of thermodynamic conditions and geometries typical of PWR and BWR fuel assemblies as well as pipes up to 450 mm in diameter, (3) the applicability to various fluid types (steam–water, air–water, hydrocarbons and oxygen), and (4) the continuous function against the void fraction. The correlation set is given as follows.

The distribution parameter is expressed as

$$C_0=F_rC_{0v}+(1-F_r)C_{0h} \quad (56)$$

where C_{0v} and C_{0h} are the concentration parameters evaluated for vertical and horizontal flows and F_r is the flow orientation parameter defined by

for $Re_g\geq 0$

$$F_r=(90^\circ-\theta_v)/90^\circ,\quad \text{for } 0^\circ\leq\theta_v\leq 90^\circ \quad (57)$$

for $Re_g<0$

$$F_r=\begin{cases}1, & \text{for } \theta_v<80^\circ\\ (90^\circ-\theta_v)/10^\circ, & \text{for } 80^\circ\leq\theta_v\leq 90^\circ\end{cases} \quad (58)$$

where θ_v is the pipe orientation angle measured from the vertical axis. The gas Reynolds number, Re_g, is defined by

$$Re_g\equiv\frac{\rho_g\langle j_g\rangle D_H}{\mu_g} \quad (59)$$

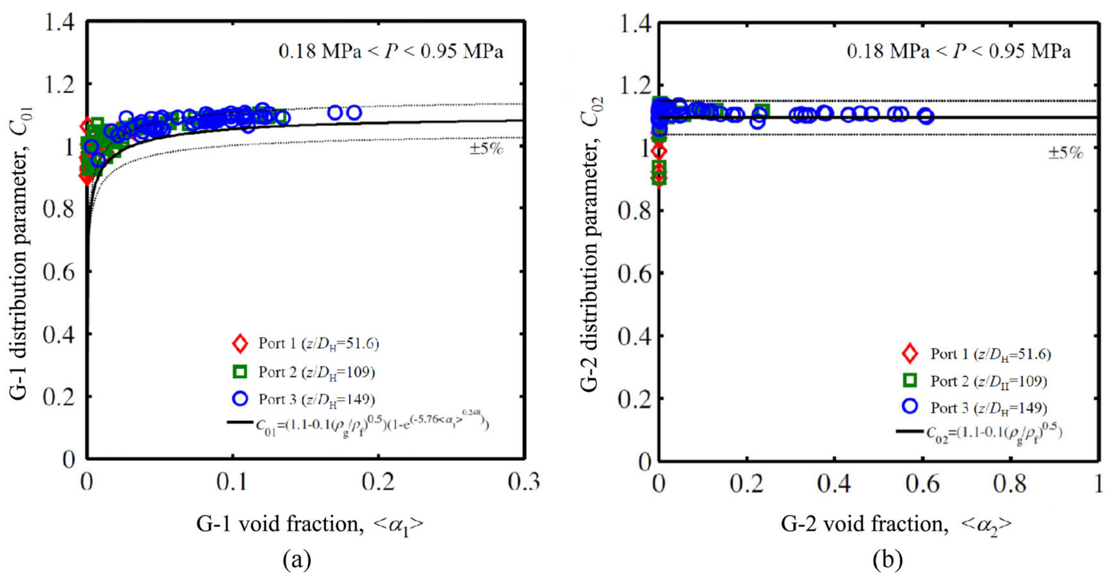

Fig. 8 Validation of boiling distribution parameter correlations for (a) group-1 bubbles and (b) group-2 bubbles in annulus channels (Brooks et al., 2012b; reproduced with permission © Elsevier Ltd. 2012).

where μ_g is the gas viscosity.

The concentration parameter for vertical flow is represented as follows:

for $Re_g \geq 0$

$$C_{0v} = L/[K_0 + (1-K_0)\langle\alpha\rangle^r] \quad (60)$$

for $Re_g < 0$

$$C_{0v} = \max\begin{cases} L/[K_0 + (1-K_0)\langle\alpha\rangle^r] \\ V_{gj}^{\circ}(1-\langle\alpha\rangle)^{0.2}/(|\langle j_g\rangle| + |\langle j_f\rangle|) \end{cases} \quad (61)$$

where L is the Chexal–Lellouche fluid parameter given as follows:

for steam–water

$$L = \frac{1-\exp(-C_1\langle\alpha\rangle)}{1-\exp(-C_1)} \quad (62)$$

for air–water

$$L = \begin{cases} \min(1.15\langle\alpha\rangle^{0.45}, 1.0), & \text{for } Re_g \geq 0 \\ \min(1.05\langle\alpha\rangle^{0.25}, 1.0), & \text{for } Re_g < 0 \end{cases} \quad (63)$$

for refrigerant

$$L = \begin{cases} \langle\alpha\rangle^{0.025(1+10\langle\alpha\rangle)}\exp[0.5(1-\langle\alpha\rangle)], & \text{for } Re_g \geq 0 \\ [1-\exp(-100\langle\alpha\rangle)][0.02(\langle\alpha\rangle + 4) \\ \quad - 0.074\langle\alpha\rangle^2(1-\langle\alpha\rangle)], & \text{for } Re_g < 0 \end{cases} \quad (64)$$

Here,

$$C_1 = 4p_{crit}^2/[p(p_{crit} - p)] \quad (65)$$

$$K_0 = B_1 + (1-B_1)(\rho_g/\rho_f)^{1/4} \quad (66)$$

$$r = (1.0 + 1.57\rho_g/\rho_f)/(1-B_1) \quad (67)$$

$$B_1 = \min(0.8, A_1) \quad (68)$$

$$A_1 = 1/[1+\exp(-Re/60000)] \quad (69)$$

$$Re = \begin{cases} Re_g, & \text{if } Re_g > Re_f \text{ or } Re_g < 0 \\ Re_f, & \text{if } Re_g \leq Re_f \end{cases} \quad (70)$$

$$Re_f \equiv \frac{\rho_f\langle j_f\rangle D_H}{\mu_f} \quad (71)$$

where $\langle j_f\rangle$ and μ_f are the area-averaged superficial liquid velocity and liquid viscosity, respectively.

The concentration parameter for horizontal flow is represented as follows:

$$C_{0h} = [1 + \langle\alpha\rangle^{0.05}(1-\langle\alpha\rangle)^2]C_{0v} \quad (72)$$

where C_{0v} is defined by Eq. (60) with the Chexal–Lellouche fluid parameter given as follows:

for steam–water

$$L = \frac{1-\exp(-C_1\langle\alpha\rangle)}{1-\exp(-C_1)} \quad (73)$$

for air–water

$$L = \min(1.25\langle\alpha\rangle^{0.6}, 1.0) \quad (74)$$

for refrigerant

$$L = \langle\alpha\rangle[1.375 - 1.5(\langle\alpha\rangle - 0.5)^2] \quad (75)$$

The drift velocity for co-current upward flow and pipe orientation angles ($0^\circ < \theta_v < 90^\circ$) is expressed as

$$\langle\langle v_{gj}\rangle\rangle = FrV_{gjv} + (1-Fr)V_{gjh} \quad (76)$$

where V_{gjv} and V_{gjh} are the drift velocities for vertical and horizontal flows, respectively. The drift velocity for co-current downward flow is expressed as

$$\langle\langle v_{gj}\rangle\rangle = FrV_{gjv} + (Fr-1)V_{gjh} \quad (77)$$

The drift velocity for a vertical pipe covers co-current upward and downward flows and counter-current flow and is given by

$$V_{gjv} = V_{gj}^{\circ}C_g \quad (78)$$

where

$$V_{gj}^{\circ} = 1.41\left(\frac{\Delta\rho g\sigma}{\rho_f^2}\right)^{0.25} C_2C_3C_4 \quad (79)$$

$$C_g = \begin{cases} (1-\langle\alpha\rangle)^{B_1}, & \text{for } Re_g \geq 0 \\ \min(0.7, (1-\langle\alpha\rangle)^{0.65}), & \text{for } Re_g < 0 \end{cases} \quad (80)$$

$$C_2 = \begin{cases} 0.4757[\ln(\rho_f/\rho_g)]^{0.7}, & \text{for } (\rho_f/\rho_g) \leq 18 \\ 1 \text{ if } C_5 \geq 1, \quad 1/\{1-\exp[-C_5/(1-C_5)]\} \text{ if } C_5 < 1, \\ & \text{for } Re_g < 0 \end{cases} \quad (81)$$

$$C_5 = \sqrt{150/(\rho_f/\rho_g)} \quad (82)$$

$$C_4 = \begin{cases} 1, \text{ if } C_7 \geq 1 \\ 1/[1-\exp(-C_8)], \text{ if } C_7 < 1 \end{cases} \quad (83)$$

$$C_7 = (D_2/D_H)^{0.6} \quad (84)$$

$$C_8 = \frac{C_7}{1-C_7} \quad (85)$$

$$D_2 = 0.09144 \text{ m (normalizing diameter)} \quad (86)$$

For upward flow (both $\langle j_g \rangle$ and $\langle j_f \rangle$ are positive)

$$C_3 = \max\begin{cases} 0.50 \\ 2\exp\left(-|Re_f|/60000\right) \end{cases} \tag{87}$$

For downward flow (both $\langle j_g \rangle$ and $\langle j_f \rangle$ are negative)

$$C_3 = 2\left(C_{10}/2\right)^{B_2} \tag{88}$$

$$C_{10} = 2\exp\left(-\frac{|Re_f|}{350000}\right)^{0.4} - 1.75(|Re_f|)^{0.03}\exp\left[-\frac{|Re_f|}{50000}\left(\frac{D_1}{D_H}\right)^2\right] + |Re_f|^{0.001}\left(\frac{D_1}{D_H}\right)^{0.25} \tag{89}$$

$$B_2 = \left\{1/\left[1+0.05\left(|Re_f|/350000\right)\right]\right\}^{0.4} \tag{90}$$

$$D_1 = 0.0381 \text{ m (normalizing diameter)} \tag{91}$$

For counter-current flow ($\langle j_g \rangle$ is positive and $\langle j_f \rangle$ is negative)

On the counter-current flooding limit (CCFL) line

$$C_3 = 2\left(C_{10}/2\right)^{B_2} \tag{92}$$

In the region of counter-current flow, there are two solutions for the void fraction, $\langle \alpha_1 \rangle$ and $\langle \alpha_2 \rangle$, at every point. The desired void fraction, $\langle \alpha_{des} \rangle$, known a priori from pressure drop or other information must be used in selecting the appropriate C_3 as follows:

$$C_3 = 2\left(C_{10}/2\right)^{B_2} \quad \text{for } \langle \alpha_{des} \rangle = \max(\langle \alpha_1 \rangle, \langle \alpha_2 \rangle) \tag{93}$$

$$C_3 = \min\begin{cases} 2\left(C_{10}/2\right)^{B_2}\left(\langle j_f \rangle/\langle j_f^* \rangle\right) \\ \quad + 2\left(1+|Re_f|/60000\right)\left(1-\langle j_f \rangle/\langle j_f^* \rangle\right) \\ 2\left(C_{10}/2\right)^{B_2} \end{cases} \quad \text{for } \langle \alpha_{des} \rangle = \min(\langle \alpha_1 \rangle, \langle \alpha_2 \rangle) \tag{94}$$

where $\langle j_f^* \rangle$ is the value on the CCFL line corresponding to $\langle j_g \rangle$ and is calculated using Eq. (92).

The drift velocity for horizontal flow is evaluated with Eq. (78) as used for vertical flows, using positive values of the superficial velocities. The applicable range of Chexel–Lellouche correlation is tabulated in Table 1.

5.2 Bhagwat–Ghajar correlation

The unique features of the Bhagwat–Ghajar correlation (2014) are (1) the independence on flow regime, (2) the applicability to the wide range of thermodynamic conditions and geometries (circular, annular, and rectangular channels) as well as pipes up to 305 mm in diameter, (3) the applicability to various fluid types (steam–water, gas–water, refrigerants and air–oil), and (4) the continuous function against the void fraction. The correlation set is given as follows.

The distribution parameter is expressed as

$$C_0 = \frac{2-\left(\rho_g/\rho_f\right)^2}{1+\left(Re_{tp}/1000\right)^2} + \frac{\left\{\left[1+\left(\rho_g/\rho_f\right)^2\cos\theta_h\right]/\left(1+\cos\theta_h\right)\right\}^{\frac{1-\langle\alpha\rangle}{5}} + C_{0,1}}{1+\left(Re_{tp}/1000\right)^2} \tag{95}$$

where θ_h is the pipe orientation angle measured from the horizontal axis. The two-phase mixture Reynolds number is defined by

$$Re_{tp} \equiv \frac{\rho_f \langle j \rangle D_H}{\mu_f} \tag{96}$$

The parameter, $C_{0,1}$, is defined by

$$C_{0,1} = (C_1 - C_1\sqrt{\rho_g/\rho_f})[(2.6-\langle j_g \rangle/\langle j \rangle)^{0.15} - \sqrt{f_{tp}}](1-x)^{1.5} \tag{97}$$

where the constant, C_1, is 0.2 for circular and annular channels and 0.4 for a rectangular channel and x is the two-phase flow quality. For horizontal and near horizontal channel orientations, Bhagwat and Ghajar recommended

Table 1 Applicable range of Chexel–Lellouche correlation (Chexel et al., 1991)

	Void fraction	Mass velocity (kg/(m²·s))	Pressure (bar)	Heat flux (kW/m²)	Subcooling (K)	Geometry
Diabatic steam–water	0.01–0.95	0.01–2100	1–145	1.3–1130	0–30	Bundle and tube (D_H = 9–48 mm)
Adiabatic steam–water	0.05–0.98	0.01–2550	1–180	N/A	N/A	Tube (D_H = 5–456 mm)
Air–water	0.01–0.98	0.04–5500	1–6.8	N/A	N/A	Tube and channel (D_H = 10–300 mm)
Refrigerant (R11, R12, R22, R113, R114, oxygen)	0.01–0.99	70–4100	1–23	N/A	N/A	Tube (D_H = 30–120 mm)

the following equation:

$$C_{0,1} = 0 \quad \left(0^\circ \geq \theta_h \geq -50^\circ \text{ and } Fr_g \leq 0.1\right) \tag{98}$$

where

$$Fr_g \equiv \frac{\langle j_g \rangle}{\sqrt{\dfrac{\Delta\rho g D_H \cos\theta_h}{\rho_g}}} \tag{99}$$

The two-phase Fanning friction factor, f_{tp}, is calculated using Colebrook equation (1939) as

$$\frac{1}{\sqrt{f_{tp}}} = -4.0\log_{10}\left(\frac{\varepsilon/D_H}{3.7} + \frac{1.256}{Re_{tp}\sqrt{f_{tp}}}\right) \tag{100}$$

where ε is the wall surface roughness.

The drift velocity is expressed by

$$\langle\langle v_{gj}\rangle\rangle = (0.35\sin\theta_h + 0.45\cos\theta_h)\sqrt{\frac{\Delta\rho g D_H}{\rho_f}}(1-\langle\alpha\rangle)^{0.5} C_2 C_3 C_4 \tag{101}$$

where

$$C_2 = \begin{cases} \left[\dfrac{0.434}{\log_{10}(\mu_f/0.001)}\right]^{0.15}, & (\mu_f/0.001) > 10 \\ 1, & (\mu_f/0.001) \leq 10 \end{cases} \tag{102}$$

$$C_3 = \begin{cases} \left(\dfrac{N_{La}}{0.025}\right)^{0.9}, & N_{La} < 0.025 \\ 1, & N_{La} \geq 0.025 \end{cases} \tag{103}$$

$$C_4 = \begin{cases} 1, & \text{other than } 0^\circ \geq \theta_h \geq -50^\circ \text{ and } Fr_g \leq 0.1 \\ -1, & 0^\circ \geq \theta_h \geq -50^\circ \text{ and } Fr_g \leq 0.1 \end{cases} \tag{104}$$

The non-dimensional Laplace length is defined by

$$N_{La} \equiv \frac{\sqrt{\sigma/\Delta\rho g}}{D_H} \tag{105}$$

The applicable range of Bhagwat–Ghajar correlation covers the two-phase Reynolds number from 10 to 5×10^6, pressure from 0.1 to 18.1 MPa, liquid viscosity from 0.0001 to 0.6 Pa·s, hydraulic equivalent diameter from 0.5 to 305 mm (circular, rectangular, and annular channels), and pipe orientation of $-90^\circ \leq \theta_h \leq 90^\circ$. The fluid systems used for the validation are air–water, argon–water, natural gas–water, air–kerosene, air–glycerin, argon–acetone, argon–ethanol, argon–alcohol, refrigerants (R11, R12, R22, R134a, R114, R410A, R290, and R1234yf), steam–water, and air–oil fluid combinations.

6 Conclusions

The drift-flux parameters such as distribution parameter and drift velocity are critical parameters in the one-dimensional two-fluid model used in nuclear thermal-hydraulic system analysis codes. These parameters affect the drag force acting on the gas phase. The accurate prediction of the drift-flux parameters is indispensable to the accurate prediction of the void fraction. Because of this, the current paper conducted a state-of-the-art review on one-dimensional drift-flux correlations for various flow channel geometries and flow orientations. Section 2 described the formulation of the one-dimensional drift-flux model and interfacial drag force using the two drift-flux parameters. Section 3 reviewed the state-of-the-art constitutive equations of the one-dimensional drift-flux model for two-phase flow in various medium-size channels. The covered flow conditions and channel geometries were upward two-phase flow in vertical circular, rectangular and annulus channels and vertical sub-channel of the rod bundle, horizontal two-phase flow in a circular channel, and downward two-phase flow in a circular channel. The essential conclusions in Section 3 were:

- A channel geometry affected the distribution parameter.
- A boundary condition (adiabatic or diabatic) affected the distribution parameter in a bubbly flow.
- The drift velocity for a horizontal channel was approximated to be zero.

The distribution parameter developed for a circular channel was not a good approximation to calculate the distribution parameter for a sub-channel of the rod bundle. It should be noted here that this approximation was often used in thermal-hydraulic system analysis codes.

Section 4 covered a newly proposed concept of the two-group drift-flux model to provide the constitutive equation to close the modified gas mixture momentum equation mathematically. The covered flow conditions and channel geometry were upward adiabatic and boiling two-phase flow in annulus channels. Because of the similarity in the distribution parameter between annulus channel and sub-channel of the rod bundle, the constitutive equations for the annulus channel could be used for calculating the distribution parameter of a sub-channel of the rod bundle as a first approximation.

Section 5 described the existing drift-flux correlations applicable to a full range of void fraction. They were Chexel–Lellouche correlation and Bhagwat–Ghajar correlation. These correlations used many empirical constants and branches. The correlations were not explicit correlations for the void fraction, and some iterations were required for obtaining the solution of the void fraction. Due to their empirical nature, the correlations should be used within the validated range.

References

Abbs, T., Hibiki, T. 2019. One-dimensional drift-flux correlation for vertical upward two-phase flow in a large size rectangular channel. *Prog Nucl Energ*, 110: 311–324.

Andersen, J. G. M., Chu, K. H. 1982. BWR refill-reflood program task 4.7: Constitutive correlations for shear and heat transfer for the BWR version of TRAC (No. NUREG/CR--2134). General Electric Co.

Bajorek, S. 2008. TRACE/V5.0 theory manual; field equations, solutions methods, and physical models. United States Nuclear Regulatory Commission.

Baotong, S., Rassame, S., Nilsuwankosit, S., Hibiki, T. 2019. Drift-flux correlation of oil–water flow in horizontal channels. *J Fluid Eng*, 141: 031301.

Barnea, D., Shoham, O., Taitel, Y., Dukler, A. E. 1980. Flow pattern transition for gas–liquid flow in horizontal and inclined pipes. Comparison of experimental data with theory. *Int J Multiphase Flow*, 6: 217–225.

Bhagwat, S. M., Ghajar, A. J. 2014. A flow pattern independent drift flux model based void fraction correlation for a wide range of gas–liquid two phase flow. *Int J Multiphase Flow*, 59: 186–205.

Borkowski, J. A., Wade, N. L., Rouhani, S. Z., Shumway, R. W., Weaver, W. L., Rettig, W. H., Kullberg, C. L. 1992. TRAC-BF1/MOD1 models and correlations (No. NUREG/CR--4391). Nuclear Regulatory Commission.

Brooks, C. S., Hibiki, T., Ishii, M. 2012a. Interfacial drag force in one-dimensional two-fluid model. *Prog Nucl Energ*, 61: 57–68.

Brooks, C. S., Ozar, B., Hibiki, T., Ishii, M. 2012b. Two-group drift-flux model in boiling flow. *Int J Heat Mass Transfer*, 55: 6121–6129.

Brooks, C. S., Paranjape, S. S., Ozar, B., Hibiki, T., Ishii, M. 2012c. Two-group drift-flux model for closure of the modified two-fluid model. *Int J Heat Fluid Flow*, 37: 196–208.

Chexal, B., Lellouche, G., Horowitz, J., Healzer, J., Oh, S. 1991. The Chexal–Lellouche void fraction correlation for generalized applications. Nuclear Safety Analysis Center of the Electric Power Research Institute, USA.

Chuang, T. J., Hibiki, T. 2015. Vertical upward two-phase flow CFD using interfacial area transport equation. *Prog Nucl Energ*, 85: 415–427.

Chuang, T. J., Hibiki, T. 2017. Interfacial forces used in two-phase flow numerical simulation. *Int J Heat Mass Transfer*, 113: 741–754.

Colebrook, C. F. 1939. Turbulent flow in pipes, with particular reference to the transition region between the smooth and rough pipe laws. *J Inst Civ Eng*, 11: 133–156.

Goda, H., Hibiki, T., Kim, S., Ishii, M., Uhle, J. 2003. Drift-flux model for downward two-phase flow. *Int J Heat Mass Transfer*, 46: 4835–4844.

Grossetete, C. 1995. Caractérisation expérimentale et simulations de l'évolution d'un écoulement diphasique à bulles ascendant dans une conduite vertical. Ph.D. Thesis. Châtenay-Malabry, Ecole centrale de Paris, France.

Hibiki, T., Ishii, M. 1999. Experimental study on interfacial area transport in bubbly two-phase flows. *Int J Heat Mass Transfer*, 42: 3019–3035.

Hibiki, T., Ishii, M. 2002a. Distribution parameter and drift velocity of drift-flux model in bubbly flow. *Int J Heat Mass Transfer*, 45: 707–721.

Hibiki, T., Ishii, M. 2002b. Interfacial area concentration of bubbly flow systems. *Chem Eng Sci*, 57: 3967–3977.

Hibiki, T., Ishii, M. 2003. One-dimensional drift-flux model for two-phase flow in a large diameter pipe. *Int J Heat Mass Transfer*, 46: 1773–1790.

Hibiki, T., Ishii, M. 2009. Interfacial area transport equations for gas–liquid flow. *J Comput Multiphase Flows*, 1: 1–22.

Hibiki, T., Ishii, M., Xiao, Z. 2001. Axial interfacial area transport of vertical bubbly flows. *Int J Heat Mass Transfer*, 44: 1869–1888.

Hibiki, T., Mishima, K. 2001. Flow regime transition criteria for upward two-phase flow in vertical narrow rectangular channels. *Nucl Eng Des*, 203: 117–131.

Hibiki, T., Ozaki, T. 2017. Modeling of void fraction covariance and relative velocity covariance for upward boiling flow in vertical pipe. *Int J Heat Mass Transfer*, 112: 620–629.

Hibiki, T., Rong, S. T., Ye, M., Ishii, M. 2003. Modeling of bubble-layer thickness for formulation of one-dimensional interfacial area transport equation in subcooled boiling two-phase flow. *Int J Heat Mass Transfer*, 46: 1409–1423.

Hibiki, T., Schlegel, J. P., Ozaki, T., Miwa, S., Rassame, S. 2018. Simplified two-group two-fluid model for three-dimensional two-phase flow computational fluid dynamics for vertical upward flow. *Prog Nucl Energ*, 108: 503–516.

Information System Laboratories. 2001. RELAP5/MOD3.3 code manual volume IV: Models and correlations. US NRC (NUREG/CR-5535/Rev 1-Vol.IV).

Ishii, M. 1977. One-dimensional drift-flux model and constitutive equations for relative motion between phases in various two-phase flow regimes. Report No. ANL-77-47. Argonne National Laboratory, USA,

Ishii, M., Hibiki, T. 2010. *Thermo-Fluid Dynamics of Two-Phase Flow*, 2nd edn. Springer Science & Business Media.

Ishii, M., Mishima, K. 1984. Two-fluid model and hydrodynamic constitutive relations. *Nucl Eng Des*, 82: 107–126.

Julia, J. E., Hibiki, T. 2011. Flow regime transition criteria for two-phase flow in a vertical annulus. *Int J Heat Fluid Flow*, 32: 993–1004.

Julia, J. E., Hibiki, T., Ishii, M., Yun, B. J., Park, G. C. 2009. Drift-flux model in a sub-channel of rod bundle geometry. *Int J Heat Mass Transfer*, 52: 3032–3041.

Kalkach-Navarro, S. 1992. The mathematical modeling of flow regime transition in bubbly two-phase flow. Ph.D. Thesis. Rensselaer Polytechnic Institute, USA.

Kataoka, I., Ishii, M. 1987. Drift flux model for large diameter pipe and new correlation for pool void fraction. *Int J Heat Mass Transfer*, 30: 1927–1939.

Kondo, M., Kumamaru, H., Murata, H., Anoda, Y., Kukita, Y. 1993. Core void fraction distribution under high-temperature high-pressure boil-off conditions (No. JAERI-M-93-200). Japan Atomic Energy Research Institute.

Liu, H., Hibiki, T. 2017. Flow regime transition criteria for upward two-phase flow in vertical rod bundles. *Int J Heat Mass Transfer*, 108: 423–433.

Liu, H., Pan, L. M., Hibiki, T., Zhou, W. X., Ren, Q. Y., Li, S. S. 2018. One-dimensional interfacial area transport for bubbly two-phase flow in vertical 5×5 rod bundle. *Int J Heat Fluid Flow*, 72: 257–273.

Liu, T. T. 1989. Experimental investigation of turbulence structure in two-phase bubbly flow. Ph.D. Thesis. Northwestern University, USA.

Lokanathan, M., Hibiki, T. 2018. Flow regime transition criteria for co-current downward two-phase flow. *Prog Nucl Energ*, 103: 165–175.

Marchaterre, J. F. 1956. The effect of pressure on boiling density in multiple rectangular channels (Report No. ANL-5522). Argonne National Laboratory, USA.

Mishima, K., Ishii, M. 1984. Flow regime transition criteria for upward two-phase flow in vertical tubes. *Int J Heat Mass Transfer*, 27: 723–737.

Morooka, S. I., Yoshida, H., Inoue, A., Oishi, M., Aoki, T., Nagaoka, K. 1991. In-bundle void measurement of BWR fuel assembly by X-ray CT scanner. In: Proceedings of the 1st JSME/ASME Joint International Conference on Nuclear Engineering, Paper No. 38.

Ozaki, T., Hibiki, T. 2015. Drift-flux model for rod bundle geometry. *Prog Nucl Energ*, 83: 229–247.

Ozaki, T., Hibiki, T. 2018. Modeling of distribution parameter, void fraction covariance and relative velocity covariance for upward steam-water boiling flow in vertical rod bundle. *J Nucl Sci Tech*, 55: 386–399.

Ozaki, T., Suzuki, R., Mashiko, H., Hibiki, T. 2013. Development of drift-flux model based on 8×8 BWR rod bundle geometry experiments under prototypic temperature and pressure conditions. *J Nucl Sci Tech*, 50: 563–580.

Ozar, B., Dixit, A., Chen, S. W., Hibiki, T., Ishii, M. 2012. Interfacial area concentration in gas–liquid bubbly to churn-turbulent flow regime. *Int J Heat Fluid Flow*, 38: 168–179.

Ozar, B., Jeong, J. J., Dixit, A., Julia, J. E., Hibiki, T., Ishii, M. 2008. Flow structure of gas–liquid two-phase flow in an annulus. *Chem Eng Sci*, 63: 3998–4011.

Rassame, S., Hibiki, T. 2018. Drift-flux correlation for gas–liquid two-phase flow in a horizontal pipe. *Int J Heat Fluid Flow*, 69: 33–42.

Serizawa, A., Kataoka, I., Michiyoshi, I. 1991. Phase distribution in bubbly flow. In: *Multiphase Science and Technology, Vol. 6*. Hewitt, G. F., Delhaye, J. M., Zuber, N. Eds. Hemisphere, 257–301.

Taitel, Y., Bornea, D., Dukler, A. E. 1980. Modelling flow pattern transitions for steady upward gas–liquid flow in vertical tubes. *AIChE J*, 26: 345–354.

Vaidheeswaran, A., Hibiki, T. 2017. Bubble-induced turbulence modeling for vertical bubbly flows. *Int J Heat Mass Transfer*, 115: 741–752.

Yang, X., Schlegel, J. P., Liu, Y., Paranjape, S., Hibiki, T., Ishii, M. 2012. Measurement and modeling of two-phase flow parameters in scaled 8×8 BWR rod bundle. *Int J Heat Fluid Flow*, 34: 85–97.

Zuber, N., Findlay, J. A. 1965. Average volumetric concentration in two-phase flow systems. *J Heat Transfer*, 87: 453–468.